Available online at www.sciencedirect.com

ScienceDirect

Journal of Nutritional Biochemistry 152 (2026) 110285

Journal of Nutritional Biochemistry

RESEARCH PAPER

Placental morphofunctional adaptations and offspring outcomes after protein restriction before and during pregnancy in mice

Fernando Felicioni[a,#], José Andrés Nivia-Riveros[a,#], Andre Lucas Caldeira-Brant[a,b], Thais de Mérici Domingues e Paula[a], Lucas Carvalho Cardoso[a], Camila Ferreira Sales[a], Julia Meireles Nogueira[a], Ana Maria Alvarenga Fagundes[a], Elizete Rizzo[a], Hélio Chiarini-Garcia[a], Erika Cristina Jorge[a], Enrrico Bloise[a], Fernanda Radicchi Campos Lobato de Almeida[a,*]

[a] Department of Morphology, Institute of Biological Sciences, Federal University of Minas Gerais, Belo Horizonte, Minas Gerais, Brazil
[b] Department of Biomedicine, Institute of Biological Sciences and Health, Catholic Pontifical University of Minas Gerais, Belo Horizonte, Minas Gerais, Brazil

Received 3 July 2025; received in revised form 21 January 2026; accepted 23 January 2026

Abstract

Proper fetal development depends on maternal nutrition. We investigated the placental morphofunctional adaptations to a low-protein diet, and their impact on fetal and newborn outcomes. Swiss mice were fed either normal (NPD, 20% crude protein, n=29) or low protein (LPD, 8% crude protein, n=26) diets two weeks before and throughout pregnancy. Dams were euthanized at gestational days (GD) 7.5 and 17.5 for morphological and molecular evaluations. No biometrical or histological alterations were observed in embryonic sites in both GDs. However, LPD placentae exhibited 14.2% increase in maternal sinusoid and 8% reduction in fetal vessel proportions ($P<.05$), without significant changes in cellular proliferation, or apoptosis. Placental gene expression analysis varied according to uterine location: LPD placentae near the ovary exhibited downregulation of *Fatp4, Mtor*, and *Kiss1*, while *Stat3* was upregulated ($P<.05$); in the middle third of the uterine horn, *Snat1* and *Kiss1* were upregulated, while *Snat4* was downregulated ($P<.05$); and close to the uterine body, *Igf2r* was downregulated, whereas *Snat1* and *Kiss1r* were upregulated ($P<.05$), suggesting region-specific compensatory mechanisms. LPD placentae and fetuses were lighter and exhibited higher brain-to-liver weight ratio in both genders ($P<.05$). Maternal LPD intake disproportionately affected male fetuses, which presented higher placental efficiency ($P<.05$), yet failed to reach their full growth potential. At birth, although newborn size was not affected by LPD, liver weights were lower and brain-to-liver weight ratios remained higher ($P<.05$), particularly in males. Maternal LPD induces region-specific placental adaptations that partially compensate for nutrient restriction, yet still impair fetal growth, particularly in male offspring.

Keywords: Low protein diet; DOHaD; Placental histomorphometry; Placental adaptation; Fetal growth; Birth weight.

1. Introduction

Since 2016, addressing malnutrition has been a key focus of global public health, following the launch of the United Nations Decade of Action on Nutrition (2016–2025). This initiative led to a partnership between the World Health Organization (WHO) and the Food and Agriculture Organization (FAO), aiming to combat global malnutrition. Despite these efforts, protein malnutrition continues to be a major health issue worldwide, particularly in low- and middle-income countries. In 2019, 148 million cases of protein-energy malnutrition (PEM) were globally reported, with the highest prevalence observed in South Asia (~57 million cases) and East Asia (~26 million), while the highest mortality rates were recorded in Sub-Saharan Africa. Projections suggest that the global burden of PEM will exceed 160 million cases by 2044, especially in Asia and Africa, raising a big concern to governmental agencies and health care providers worldwide [1].

Gestational protein requirements increase to support both maternal health and fetal growth. Protein deficiency during pregnancy may lead to anemia, pre-eclampsia, and impaired immune function, as well as intrauterine growth restriction (IUGR), low birthweight, preterm birth, and increased neonatal morbidity and mortality [2]. In this connection, inadequate protein intake is not only a concern for those facing food insecurity, but also for individuals following specific dietary patterns, such as vegetarian or vegan diets, who may lack proper nutritional guidance [3].

The placenta is the primary organ responsible for maternal-fetal interactions, adapting to changes in maternal nutritional status to ensure optimal nutrient transport for fetal growth. When

* Corresponding author at: Antônio Carlos Avenue, 6627, Belo Horizonte 31270-901, Minas Gerais, Brazil.
E-mail address: falmeida@icb.ufmg.br (F.R.C.L. de Almeida).
# Felicioni and Nivia-Riveros contributed equally to this work and share the first authorship.

https://doi.org/10.1016/j.jnutbio.2026.110285

intrauterine homeostasis is disrupted by various stressful events, pregnancy is sustained through various placental morphofunctional adaptations. For example, reductions in the junctional and labyrinth zone areas are found in response to maternal undernutrition or high-fat diet intake [4]. These adaptations highlight the placenta's ability to respond to various maternal challenges, including malnutrition, ensuring fetal survival and development.

Research on hemochorial placental adaptations to maternal low-protein diet (LPD) remains limited, particularly in genetically diverse populations and in aspects such as histomorphometry and cell turnover. Ethical constraints limit well-controlled studies on the effects of low-protein diets on key placental and fetal parameters in humans, highlighting the need for translational animal models. Such models are essential for investigating the effects of maternal protein restriction on placental function, fetal development, and subsequent offspring outcomes, particularly in genetically heterogeneous populations.

Previous studies have examined placental morphofunctional processes in response to maternal low-protein diets, primarily using inbred mouse strains. These studies have reported a reduction in labyrinth vessel length [5], impaired trophoblast differentiation [6], and smaller placentae associated with inadequate fetal growth [7]. In particular, maternal protein restriction has been shown to downregulate amino acid transporter expression, thus diminishing placental nutrient uptake. Additionally, severe protein deprivation has been associated with decreased placental perfusion and oxygen availability, which can increase fetal mortality [8–10]. Most studies on placental responses to maternal malnutrition have been conducted in inbred strains such as C57BL/6J [4,11,12], which improves reproducibility but lack genetic variability. Given the highest world distribution of protein deficiency in regions with markedly different genetic backgrounds (*e.g.* South/East Asia and in Sub-Saharan Africa), data on the effects of gestational low-protein diets in mouse strains with greater genetic diversity, better reflecting the heterogeneous genetic background of humans in these and other areas, remain limited. Notably, Tuttle et al. [13] suggested that outbred mice are more suitable for translational utility of animal models due to their genetic heterogeneity. This diversity enhances the translational relevance of findings by more closely reflecting human physiological variability, for investigating how chronic protein deficiency shapes placental development and offspring outcomes.

Therefore, we hypothesized that maternal low-protein diets induce placental morphofunctional adaptations in outbred mice, leading to changes in biometrical, histomorphometrical, and molecular parameters that influence fetal growth.

2. Material and methods

2. 1 Animals and diets

Fifty-five pubertal Swiss outbred female mice (32.5±2.0 g) were housed in a climate-controlled environment with a 12-h light/12-h dark cycle and provided *ad libitum* access to water and standard mouse chow (Nuvilab, CR-1, Quimtia, Parana, Brazil). After a 15-d adaptation period, mice were randomly assigned to one of two experimental groups: normal protein diet (NPD, n=29) or low-protein diet (LPD, n=26).

Mice were fed with either a normal protein diet (NPD; 20% crude protein, 60% carbohydrates, 8% lipids) or an isocaloric (3.7 kcal/g) low-protein diet (LPD; 8% crude protein, 70% carbohydrates, 7% lipids) (Rhoster, Sao Paulo, Brazil) for 15 d prior to breeding-to induce a chronic protein deficiency period, as described in previous studies [14,7,15]. Diet was provided to each group in pellet form, *ad libitum*. During the chronicity induction period, individual feed intake could not be monitored, as mice were housed in groups of five per cage. Consequently, daily food consumption was calculated as the average intake per cage and divided by the number of females, with measurements taken every 5 d. Moreover, vaginal smears were used to determine the phases of the estrous cycle, a non-invasive and widely accepted method [16]. Proestrus was characterized by a predominance of nucleated, round epithelial cells, whereas estrus was marked by mainly keratinized cells; both stages correspond to the follicular phase. During the luteal phase, metestrus was identified by the presence of both leukocytes and round epithelial cells, while diestrus was distinguished by a predominance of leukocytes [17,18]. The total number and duration of cycles were calculated, defining each estrous cycle as the presence of one proestrus and/or estrus [19]. At the end of the 15-d period, females were mated overnight, (total n of sires=12; 1 sire for 3 to 4 females) and the presence of a vaginal plug the following morning was considered gestational day (GD) 0.5. Throughout pregnancy, females were individually housed and maintained their respective dietary regimens. Following mating, daily food intake was individually recorded for each female on the specified days outlined in the methodology. Animals were randomly euthanized at three different reproductive stages for biometrical, histomorphometrical, and molecular evaluations: GD 7.5 (embryonic period; NPD, n=8; LPD, n=8), GD 17.5 (late fetal period; NPD, n=14; LPD, n=12), and post-parturition (newborn stage; NPD, n=7; LPD, n=6). At GD 7.5 and GD 17.5, reproductive parameters, such as pregnancy rate, litter size and pre-natal mortality were determined.

The diets were formulated based on the recommendations of the American Institute of Nutrition (AIN-93G), a standardized rodent research diet designed to support growth, pregnancy, and lactation [20]. All experimental procedures were conducted in compliance with ethical principles for animal experimentation and were approved by the Ethics Committee on Animal Experimentation of the Federal University of Minas Gerais (CEUA 290/2015).

2.2. Assessment of feed intake and maternal body weight changes

Feed intake and maternal body weight were monitored daily from the first day of dietary treatment (15 d before mating) until GD0.5, and subsequently at specific gestational stages, including embryonic (GD7.5), early fetal (GD11.5), and late fetal (GD17.5) periods. Daily feed weigh-backs were conducted to estimate feed intake throughout the experimental period, and values are expressed as mean individual consumption [14].

2.3. Sample collection, biometrical evaluation, and histological preparation

Prior to euthanasia, pregnant females (NPD= 22, LPD= 20) received an injection of heparin (125 IU/mL, 20 mg/kg, s.c.) and were anesthetized with a combination of 5% ketamine (50 mg/kg, i.m.) and 2% xylazine (20 mg/kg, i.m.). They were then fixed by perfusion through the left ventricle using Karnovsky solution [21]. Following perfusion, embryonic sites (GD7.5), fetuses and placentae (GD17.5) were carefully isolated from the uterine horns, as described by Pang et al. [22], and placentae were weighed to assess the relationship between placental and fetal weight and to calculate placental efficiency––which was calculated by dividing fetal weight/placental weight to establish the fetal to placental weight ratio [23], defined as grams of fetus produced per gram of placenta [24]. Afterwards, placentae were immersed in Karnovsky solution for 24 h at room temperature for subsequent histomorphometrical analysis. Other placentae from each experimental group were selected according to their position in the uterus (close to the ovary, middle of the uterine horn, next to the uterine body), fragments

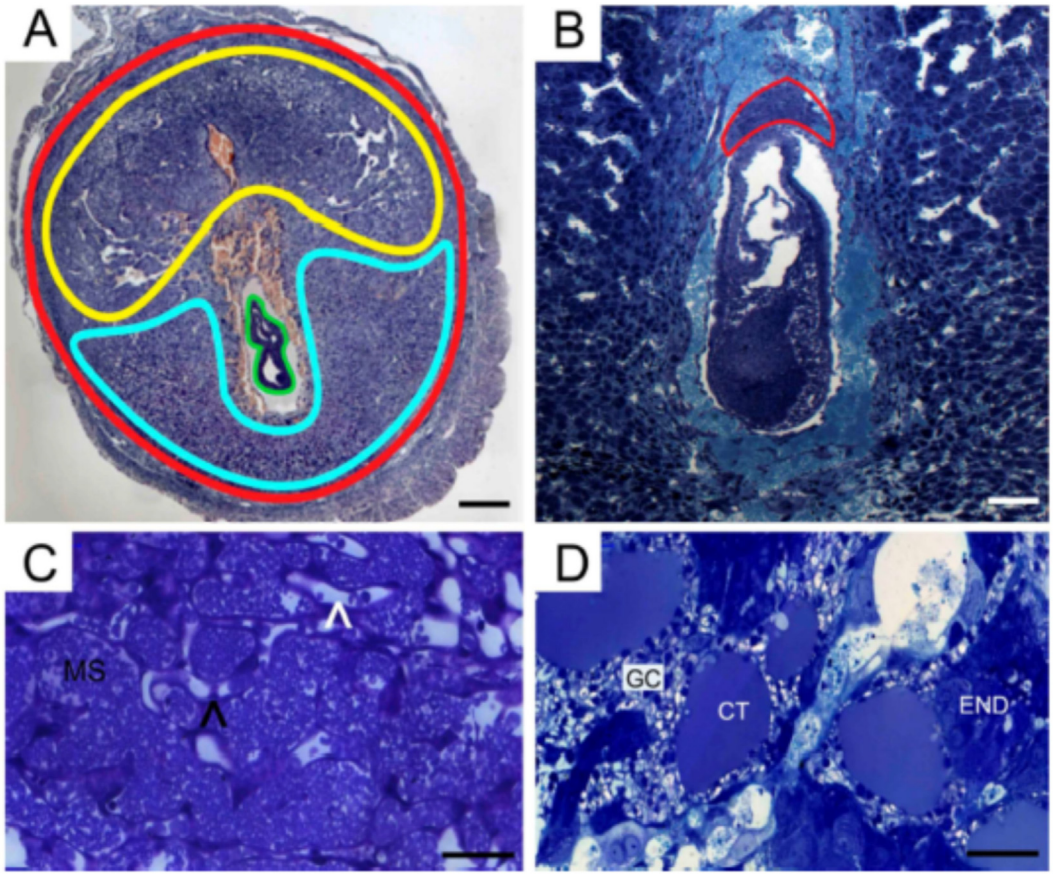

Fig. 1. Histomorphometrical evaluation of the embryonic sites (n=10 NPD, n=10 LPD). Areas of each compartment were delineated and estimated using the Pannoramic Viewer software (version 1.15.4–free version, 3D Histech) (A, B). The areas of each component of the embryonic sites and placental layer were calculated in relation to the full site/placental area. In addition, the proportions of the different histological components (C, D) of the junctional zone (glycogen cells, endocrine cells and connective tissue) and from the labyrinth-trophoblast placental layer (maternal sinusoids, interhemal membrane, and fetal vessels) were obtained by point counting. The scale bar indicates 50 μm and is representative for all photomicrographs. Abbreviations: CT, connective tissue; END, endocrine cells; GC, glycogen cells; MS, maternal sinusoid.

were collected, immersed in TRI-Reagent (Sigma-Aldrich) solution and stocked at −80°C to determine relative gene expression of nutrient transporters, metabolic and growth factors.

All fetuses and newborns were weighed, and crown-rump lengths were measured using a digital caliper. To determine the occurrence of small for gestational age (SGA) at GD17.5 and intrauterine growth restriction (IUGR) at birth, the brain and liver were weighed, and the brain-to-liver weight ratio was calculated [25]. Additionally, fetal and newborn body weight relative frequencies were analyzed in percentiles. To investigate the association between IUGR and fetal sex, fetal sex was determined using the anogenital length measurement, as described by Christiansen et al. [26].

For histomorphometrical analysis, five dams at each gestational age were randomly chosen and two embryonic sites/placentae per dam were evaluated, resulting in 10 embryonic sites at GD7.5 and 10 placentae at GD17.5 per experimental group. These tissues were embedded in glycol methacrylate plastic resin, sectioned at 3 μm thickness, and stained with toluidine blue-sodium borate, following the protocol described previously [27]. Additionally, five females from each experimental group were euthanized at GD17.5 by cervical dislocation, and their placentae were cut close to the midline, and a fragment was fixed by immersion in 4% paraformaldehyde (in 0.2M phosphate buffer, pH 7.4). These samples were then embedded in paraffin (Histosec pastilles, Merck, Darmstadt, Germany), sectioned at 5 μm thickness, for the evaluation of cellular proliferation and apoptosis.

2.4. Histomorphometrical evaluation of the maternal-fetal interface

Since the ectoplacental cone gives rise to the trophoblastic cells of the placental layers, the proportions of the compartments of the embryonic sites (Fig. 1A and B) and the different placental layers (Decidua basalis, junctional zone, labyrinth-trophoblast and chorionic plate) were evaluated. For this, the Pannoramic Viewer software (version 1.15.4–free version, 3D Histech) was used to delineate the area of each compartment using the “create polygonal or freehand annotation” tool. The “manage/locate annotations” tool was then used to obtain the area of each delineated compartment. Finally, the areas of each component of the embryonic sites and placental layer were calculated in relation to the full site/placental area (Fig. 1A and B). To assess the impact of LPD on placental morphology, the proportions of different placental layers (decidua basalis, junctional zone, labyrinth-trophoblast, and chorionic plate) were measured in two placentae per dam, selected randomly. The Pannoramic Viewer software (version 1.15.4–free version, 3D Histech) was used to delineate the area of each compartment using the “create polygonal or freehand annotation” tool. The “manage/locate annotations” tool was then used to calculate the area of each compartment. The area of each placental layer was then expressed as a percentage of the total placental area. In addition, the volumetric density (%) of different histological components within the junctional zone (glycogen cells, endocrine cells, and connective tissue) and the labyrinth-trophoblast placental layer (maternal sinusoids, interhemal membrane, and fetal

Table 1
Primers used for relative gene expression using quantitative PCR

Gene	*Forward primer*	*Reverse primer*	*Amplicon size*	*Annealing temperature*
β-actin	CTGGCTCCTAGCACCATGAAGAT	GGTGGACAGTGAGGCCAGGAT	96 bp	60°C
Snat1	CCCCCAAGACTAGAGAGGCT	GTTACCAGCACGGGAGACAA	168 bp	60°C
Snat4	TGCAATCCCAATCCTGGCTT	ATGTTGGACACCGTCTGCAT	108 bp	60°C
Glut1	GATCCCAGCAGCAAGAAGGT	TAGCCGAACTGCAGTGATCC	80 bp	60°C
Fatp4	CTGGATTCAGAGCCCTAGCG	AGGGGAGATCAGCACCTAGG	101 bp	60°C
Mtor	CGTCAATCCAGAGCACAATC	ATTTCACAATCGGAGGCAAC	225 bp	60°C
Stat3	CAGTTCTCGTCCACCACCAA	CCCAGAAGGAGAAGCCCTTG	157 bp	60°C
Igfr1	CTCATCACCCCGCATACAC	AAACCAAACCGAAAACAGGA	207 bp	60°C
Igfr2	CACCGAGAGCCACACTGATT	TTCTGGGCAGGCATAACTGG	125 bp	60°C
Kiss1	TGCTGCTTCTCCTCTGTGTC	GCGATTCCTTTTCCCAGGCA	117 bp	60°C
Kiss1r	CTGGCACCCTCGAAGCTATG	AAGTGTGAACCCAGGAAGGC	111 bp	60°C

Abbreviations: Amino acid transporter, *Snat1* (*SLC38A1*) and *Snat4* (*SLC38A4*); fatty acid transporter, Fatp4 (*SLC27A4*); glucose transporter, Glut1 (*SLC2A1*); nutrient transporter regulators in the placenta, *Mtor, Stat3 Igfr1, Igfr2*; regulation of placentation and angiogenesis, *Kiss1* and *Kiss1r*; reference gene: *β-actin*.

vessels) were determined using point counting [28,29] (Fig. 1C and D).

Ten randomly selected sections from each animal in each experimental group were analyzed under a light microscope (Olympus BX-51), with a 10x eyepiece fitted with a square lattice containing 220 intersections. A total of 10 fields per animal (resulting in 2,200 points) were randomly selected at x400 magnification. The intersections that fell on relevant structures in the tissue sections were counted by systematically moving across the grid without overlapping. The volume density of each component of the junctional zone or labyrinth-trophoblast was calculated by dividing the sum of points falling on each structure by the total number of points on the tissue sections. Results were expressed as a percentage of the junctional zone or labyrinth-trophoblast volume, calculated by multiplying the volumetric density of each component by 100.

To assess maternal-fetal exchange capacity, the thickness of the interhemal membrane was measured in 12 labyrinth-trophoblast fields from each experimental group at x100 magnification. The interhemal membrane thickness was determined using ImageJ software (version 1.49, National Institutes of Health, USA).

2.5. Evaluation of cell proliferation in the placenta

To evaluate cell proliferation, the presence of Ki67, a well-known marker for cell proliferation, was determined using immunofluorescence. All slides were stained in a single session to ensure consistency. Briefly, tissue sections were dewaxed, rehydrated, and subjected to epitope antigen retrieval by microwaving 3 times for 5 min each in 0.1M sodium citrate buffer (pH 6), followed by cooling to room temperature and rinsing with phosphate-buffered saline (PBS, pH 7.4). Analyses were performed in the placental junctional zone, labyrinth-trophoblast, and chorionic plate layers. The sections were incubated overnight at 4°C in a humidified chamber with a primary antibody against Ki67 (rabbit IgG, Abcam, ab15580) diluted 1:100 (v/v) in PBS-BSA. The following day, the sections were treated with a secondary biotin-labeled goat anti-rabbit antibody (IgG, 555 nm, A11008, Thermo Fisher Scientific) diluted 1:200 (v/v) in PBS-BSA for 90 min at 4°C. DAPI (Sigma-Aldrich, D9564; 1:1000 dilution in PBS) was used to label cell nuclei. Canine breast tumor tissue was employed as a positive and negative control for staining. Negative controls were treated without the primary antibody. Photomicrographs of stained placental tissues were captured using a Zeiss Imager Z2 microscope equipped with the Apotome Z2 image improvement system and analyzed with Zen software (blue edition, Carl Zeiss Microscopy). Cell counts were performed using the "Cell Counting" tool in ImageJ software (version 1.49–free version, National Institutes of Health, USA). The percentage of proliferating cells was calculated by dividing the number of positive Ki67-stained nuclei by the total number of nuclei (positive+negative) and multiplying by 100. The results were expressed as the percentage of proliferative cells.

2.6. Determination of cell death through DNA fragmentation–TUNEL assay

The apoptotic ratio in the placenta was assessed using the ApopTag In Situ Peroxidase Detection Kit (Merck Millipore, Merck #S7100, Carlsbad, CA, United States of America, MA, USA), following the manufacturer's guidelines. Placental sections embedded in paraffin were dewaxed with xylene, rehydrated through a series of ethanol washes, and rinsed in distilled water. To permeabilize cell membranes, the sections were treated with 0.1% Triton X-100 diluted in citrate buffer for 2 min. Next, protein digestion was performed using 1% Proteinase K in PBS buffer for 15 min. Both the junctional zone and labyrinth-trophoblast placental layers were examined using an Olympus BX51 light microscope coupled with the Q Colour3 image capture system, with images analyzed through Q Capture software (version 3, Olympus). The percentage of cell death in each placental region was calculated using the same method as for cell proliferation. The results were expressed as the percentage of cells exhibiting DNA fragmentation.

2.7. Relative gene expression analysis by quantitative PCR (qPCR)

The real-time quantitative PCR (qPCR) was performed in a Rotor Gene 3,000 Machine (Corbett Research). Relative quantifications were performed in triplicate, using β-actin as endogenous reference gene. Regarding primer design, the reference nucleotide sequences for each gene of *Mus musculus* were retrieved from the NCBI database and used as input for the Primer3Plus tool. Amplicon lengths were restricted to a range of 100–250 bp, and candidate primer pairs were generated accordingly. The designed primer pairs were subsequently evaluated using the NetPrimer tool, and only those achieving scores above 85 were selected. These primers were then subjected to sequence alignment using the BLAST tool against the NCBI database to confirm specificity and homology to the *Mus musculus* genome. Following in silico validation, the selected primer pairs were synthesized, experimentally tested, and subsequently employed in qPCR assays. The primers sequences of the genes used are given in Table 1. Total RNA isolation was per-

Table 2
Reproductive characteristics observed in female mice submitted to either a normal protein (NPD) or a low protein (LPD) diet

Reproductive parameters	NPD (n=29 dams)	LPD (n=26 dams)	*P* value
Estrous cycle duration, d	6.3±0.4	5.9±0.5	.682
Pregnancy rate %	76.0	69.0	.176
Litter size	10.7±0.5	11.0±0.5	.157
Resorbing implantation sites	0	0	-
Dead fetuses	1.8±0.4	1.0±0.5	.245

formed using TRI-Reagent (Sigma-Aldrich), following the manufacturer's instructions.

To reduce individual variations, pools with three placentas from different dams in the same treatment were performed for each uterine segment (Ov: near the ovary; M: middle portion of the uterus; Ce: close to the uterine body) (two pools per uterine segment were evaluated per treatment). This approach was used due to uterine vascularization, where it was shown that placental blood supply is provided by the ovarian artery and the uterine artery, therefor, placentae located at the edges of the uterine horns acquire more favorable growth conditions associated with blood flow [30].

From each pool, 1 μg of total RNA was converted to cDNA using the High-Capacity cDNA Reverse Transcription Kit (containing 10X RT Buffer; 10x RT Random Primers; 25x dNTP Mix (100 mM); MultiScribe Reverse Transcriptase (50 U/μL); Applied Biosystems, Foster City, CA). qPCR was conducted using 5 μL of iTAq Universal SYBR Green Supermix (Bio-Rad, Hercules, CA), 0.4 μM of each primer and 1 μL of cDNA diluted 1:10 in water and final volume adjustment to 10 μL with nuclease-free water. Thermal cycling specifications were 50°C for 2 min, 95°C for 2 min, followed by 40 cycles of 94°C for 15 s, 60°C for 30 s, 72°C for 20 s.

2.8. Statistical analysis

All variables measured were tested for normality prior to analyses, using the univariate procedure of the Statistical Analysis System (SAS Institute, 2001). This procedure also identified outliers, which were further excluded when justified. Data were analyzed as a randomized design and treatment effects on maternal feed intake, body weight changes, reproductive parameters, embryonic sites and placental histomorphometrical evaluations, proliferative and cell death percentages were analyzed using the general linear model (GLM) procedure of SAS and least square means were then compared using Student's T-test. To analyze data on maternal body weight changes, feed intake and reproductive parameters, dam was the experimental unit. Moreover, the analysis of body weight changes throughout the experimental period included the effects of treatment in the model with body weight at the beginning of treatment (w0) as covariate.

All offspring data were also analyzed as randomized design, and the complete model included treatment and sex as the main effects, and their interaction. Data were analyzed using the general linear model (GLM) procedure of SAS. If significant treatment effects were established, multiple comparisons were performed using probability of differences (PDIFF) between least square means, adjusted by Tukey-Kramer. The frequency of fetal and newborn body weights by gender in each experimental group was compared by the Chi-Square test.

The Rest 2009 software was used for the relative gene expression quantification [31]. A pairwise fixed reallocation randomization test was performed, and results were based on primer efficiency.

In all statistical analysis performed, $P<.05$ was considered significant. In the tables and figures, data are reported as least square means and the pooled standard error of the mean (SEM).

3. Results

3.1. Low protein diet (LPD) intake does not affect reproductive characteristics observed in female mice

To identify whether low protein intake alter reproductive characteristics, estrous cycle was evaluated before breeding, and parameters associated with pregnancy rate and litter size during pregnancy are summarized in Table 2. No differences in estrous cycle, pregnancy rate, litter size, resorbing implantation sites and dead fetuses were observed in the low protein intake experimental group.

3.2. Low protein diet (LPD) intake impairs maternal weight gain and promotes placental morphological adaptations

During the adaptation period (Fig. 2 A and B) ($P=.404$) and the embryonic ($P=.541$) and early fetal ($P=.272$) (Fig. 3A–C) periods, no significant differences were observed in feed intake or maternal body weight changes between the NPD and LPD groups. However, by the late fetal period (GD17.5) ($P=.025$), significant differences were detected between the experimental groups. While LPD females exhibited higher overall feed intake, their net protein intake remained lower throughout pregnancy (**P**=.0001; Fig. 3A and B). This nutritional imbalance reduced maternal weight gain in the late fetal period ($P<.05$; Fig. 3C and D).

Histomorphometrical analysis performed at the embryonic (GD7.5) and fetal (GD17.5) stages are shown in Table 3**.** During early pregnancy (GD7.5), histological parameters were not affected by maternal low protein intake. Conversely, during late gestation (GD17.5), LPD placentae exhibited higher proportion of maternal sinusoids but lower fetal vessels in the labyrinth zone ($P<.05$), with no alterations in the interhemal membrane thickness ($P>.05$). The placental compartments' (decidua basalis, junctional zone, labyrinth-trophoblast and chorionic plate; Fig. 4A) areas, expressed as a percentage of the total placental area, were not affected by previous protein restriction treatment ($P>.05$; Fig. 4B).

3.3. LPD intake does not affect placental cellular proliferation and death

To identify whether gestational low protein intake alter placental cellular turnover, we used markers of proliferation (Fig. 5) and apoptosis (Fig. 6). No differences in cellular proliferation ($P=.284$; Fig. 4C), or death ($P=.643$; Fig. 4D) rates were observed in the junctional zone, labyrinth-trophoblast or chorionic plate, providing evidence of no changes in placental cell turnover.

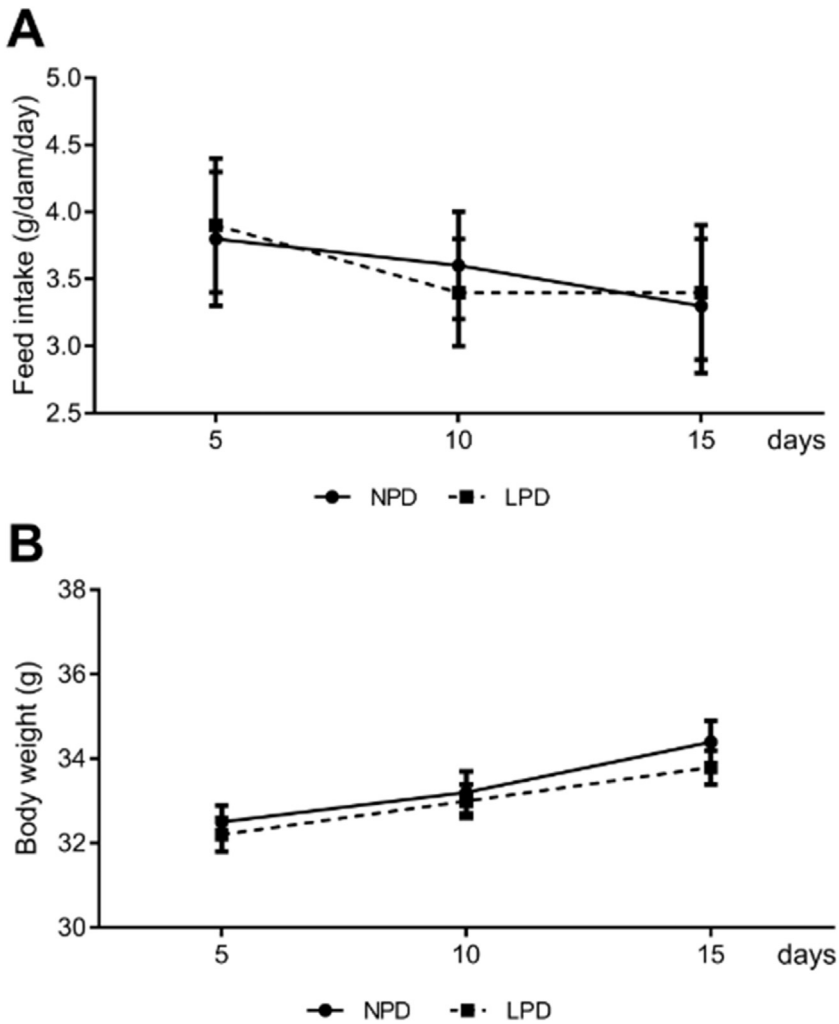

Fig. 2. Average daily feed intake (A) and body weight changes (B) in the control (NPD, n=29) and treated (LPD, n=26) experimental groups during the first day of treatment until breeding (chronic low protein intake induction period). Both diets were fed *ad libitum* and offered for two weeks before pregnancy and did not affect either feed intake or body weight at this stage ($P>.05$). Solid lines with circles and dashed lines with rectangles represent the NPD and LPD groups, respectively.

3.4. LPD intake promotes offspring intrauterine growth impairments in a sex-dependent manner

The evaluation of offspring biometrical parameters during the fetal period (GD17.5) and at birth is summarized in Table 4. During the fetal period, a significant interaction between treatment and sex was observed for placental and fetal weights, as well as the brain-to-liver weight ratio, as LPD males showed the lightest placentae and the highest brain-to-liver weight ratio, providing evidence of SGA fetuses ($P=.0001$). NPD fetuses and placentae were heavier regardless of sex, whereas LPD fetuses of both sexes exhibited a higher brain-to-liver weight ratio. Additionally, maternal LPD intake affected fetal development, as protein-restricted fetuses showed shorter crown-rump lengths. This effect was also sex-dependent, with male fetuses being longer than females ($P=.0061$). Moreover, low protein intake influenced the liver-to-body weight ratio, irrespective of sex ($P=.0003$). Interestingly, LPD placentae demonstrated greater efficiency ($P=.0015$), an effect that was even more pronounced in males ($P=.0349$). At birth, brain and liver weights, brain-to-liver weight ratio, and liver-to-body weight ratio were all affected by maternal low-protein intake, with male offspring exhibiting more pronounced impairments than females ($P=.0188$).

The analysis of body weight distribution by sex during late fetal development (GD17.5) and at birth is presented in Figure 7 A and B. In females, body weight frequency was not significantly affected by LPD ($P=.4231$; Fig. 7A). However, among male fetuses, there was a higher prevalence of LPD individuals falling below the 10th and 25th body weight percentiles, with none above the 75th percentile ($P=.0457$; Fig. 7A). This pattern changed at birth, where both male ($P=.1565$) and female ($P=.4368$) LPD newborns showed a body weight distribution similar to that of their NPD counterparts (Fig. 7B).

3.5. LPD modifies placental gene expression of nutrient transporters, metabolic and growth factors according to uterine location

Gene expression was compared between LPD and NPD placentae based on placental location within the uterus (near the ovary, middle of the uterine horns, and close to the uterine body; Fig. 8). Concerning placental location within the uterus, the placentae adopted different strategies in response to LPD or NPD treatments. When located near the ovary, LPD placentae exhibited downregulation of *Fatp4* (the *fatty acid transport protein 4*, a major fat acid transporter in the placenta), *Mtor (the mechanistic target of rapamycin;* a central nutrient sensor in the placenta*)*, and *Kiss1*

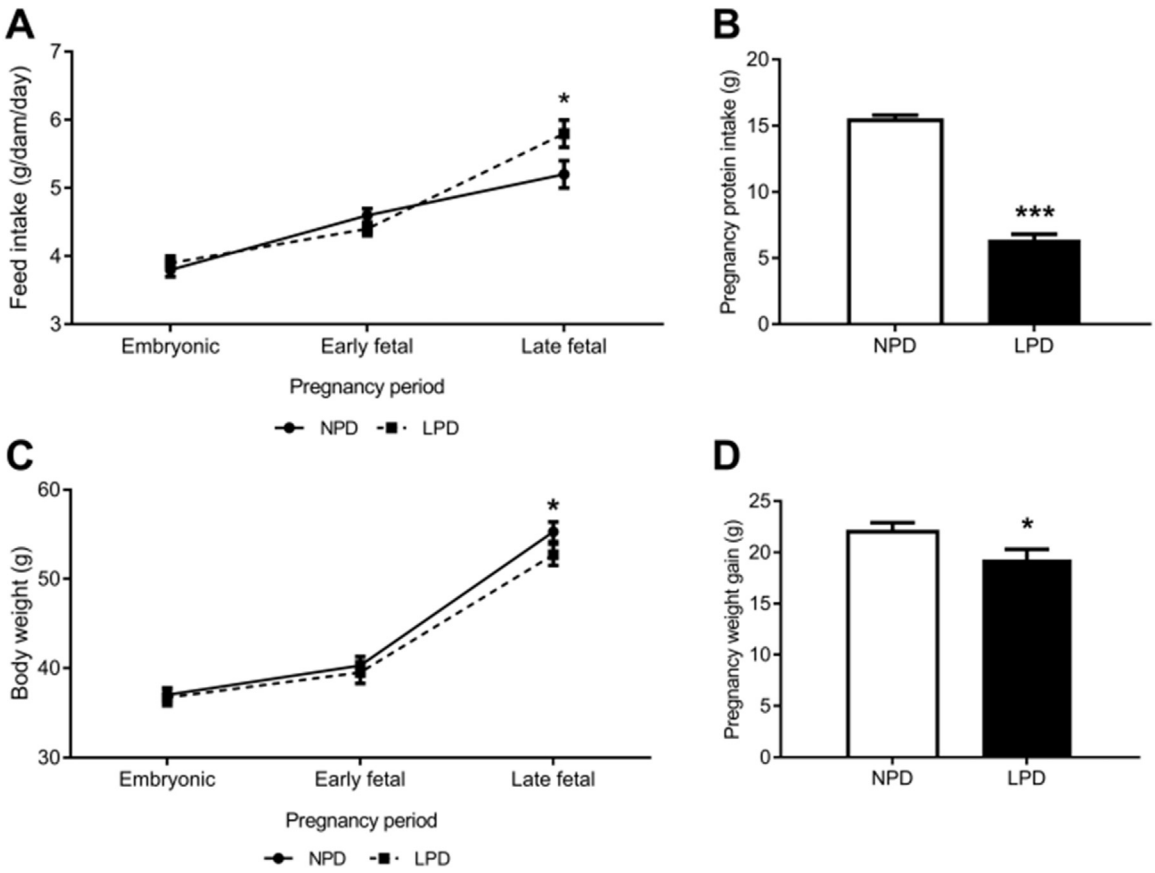

Fig. 3. Average daily feed intake (A), total protein intake (B), body weight changes (C) and body weight gain (D) throughout pregnancy in the normal (NPD, n=29) and low (LPD, n=26) protein intake experimental groups. In figures A and C, solid lines with circles and dashed lines with rectangles represent the NPD and LPD groups, respectively. In figures B and D, the white columns represent the NPD and the black columns represent the LPD groups, respectively. The experimental diets were fed *ad libitum* throughout pregnancy and feed intake was measured at three time points: early pregnancy (GD 7.5–embryonic phase), mid pregnancy (GD 11.5–early fetal phase) and late pregnancy (GD 17.5–late fetal phase). $^{*}P<.05$; $^{***}P<.001$.

Table 3
Evaluation of histological parameters in the embryonic (GD7.5–early placental development) and fetal (GD17.5–placental development accomplished) periods after maternal normal (NPD) or low (LPD) protein intake

Morphological parameters of the embryonic period (GD7.5)			
	NPD	LPD	*P*-value
Number of embryonic sites	10	10	
Embryo: site area ratio	2.45±0.25	1.70±0.35	.091
EPC: site area ratio	0.65±0.10	0.40±0.20	.206
EPC: embryo area ratio	29.5±8.40	21.6±4.70	.429
Volumetric proportion of the late fetal period (GD17.5)			
	NPD	LPD	*P*-value
Junctional Zone			
Number of placentae	10	10	
Glycogen cells	39.0±3.6	40.5±3.6	.713
Endocrine cells	46.2±2.8	44.3±2.8	.653
Connective tissue	14.8±3.0	15.1±3.0	.935
Labyrinth Zone			
Number of placentae	10	10	
Maternal sinusoids	25.2[a]±3.8	39.4[b]±3.4	.026
Interhemal membrane	52.2±3.5	46.6±3.0	.258
Fetal vessels	22.0[a]±1.3	14.0[b]±1.0	.002
Interhemal membrane thickness (μm)	1.90±0.08	1.90±0.09	.999

Abbreviation: EPC, ectoplacental cone.
[a,b] LSMeans with different superscripts letters in the same row differ ($P<.05$).

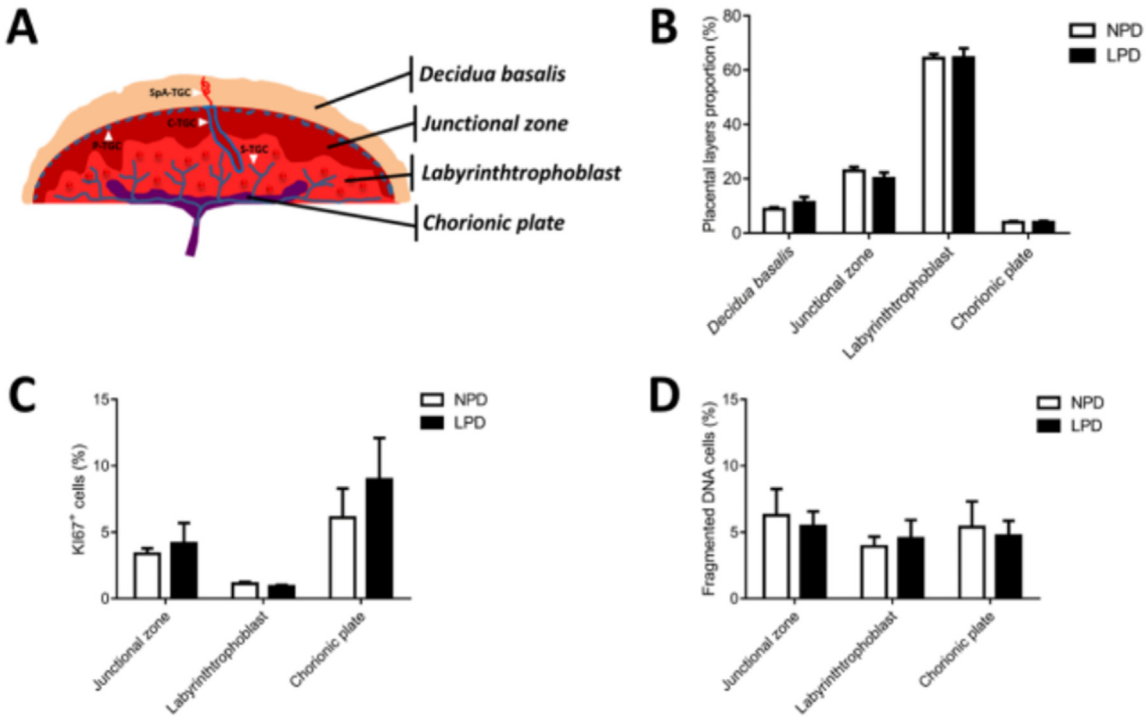

Fig. 4. Histomorphometrical and cellular evaluations of heterogenic mice placenta after chronic protein restriction. Placental layers (A), proportion of placental layers (B), percentages of cell proliferation (C) and cell death (D) were determined in normal (NPD, n=10 placentas) and low (LPD, n=10 placentas) protein intake experimental groups. All the parameters evaluated were not affected by previous nutritional treatments ($P>.05$).

(*kisspeptin*, a key regulator of placentation and angiogenesis) expressions, which was associated with upregulation of *Stat3 (Signal Transducer and Activator of Transcription 3,* a regulator of nutrient transport across the placenta), all compared to NPD placentae from the same location ($P=.0335$; Fig. 8 A and B). On the other hand, in the middle of the uterine horns, LPD placentae induced the upregulation of *Snat1 (Sodium-Coupled Neutral Amino Acid Transporter 1),* also known *as SLC38A1*, a major neutral amino acid transporter in the placenta), and *Kiss1*, accompanied by the downregulation of *Snat4*, all compared to NPD placentae from the same location ($P=.0413$; Fig. 8 C and D). Finally, when located close to the uterine body, *Igfr2 (insulin-like growth factor 2,* a regulator of resource allocation to the fetus*)* was downregulated in LPD placentae, while the expressions of *Snat1* and *Kiss1r* were upregulated in this location ($P=.0226$; Fig. 8 E and F).

4. Discussion

The present study demonstrated that LPD intake impaired maternal body weight gain during late gestation and induced placental morphological adaptations without affecting pregnancy-related parameters. Among these alterations, histological changes in LPD placentae included increased proportion of maternal sinusoids and fewer fetal vessels in the labyrinth zone, although placental cell turnover remained unchanged. Additionally, LPD exposure led to intrauterine growth impairments in a sex-dependent manner, with male fetuses experiencing greater reductions in body weight and organ development, despite the highest placental efficiency. Furthermore, LPD altered placental gene expression in a uterine location-specific manner, demonstrating different placental strategies to limit its development and increase amino acid transport. To the best of our knowledge, this is the first study to highlight specific placental adaptive strategies in response to maternal protein restriction and their implications for fetal growth and development, that are dependent on gestational-age, fetal sex, and uterine positioning of the feto-placental unit.

Significant placental alterations were observed following LPD treatment at GD 17.5, including reduced weight and size, increased proportion of maternal sinusoids, and decreased number of fetal vessels. However, LPD intake did not affect histological components proportions, cellular proliferation or apoptosis. Based on these findings, and as suggested by Díaz et al. [32], it is likely that amino acids are being preferentially directed to the fetus at the expense of placental growth. This redistribution may be linked to the impaired fetal growth observed, particularly in males, which was subsequently recovered at birth.

Overall, our findings suggest that maternal protein restriction disrupts placental nutrient-sensing and transport pathways in a manner consistent with reduced activation of trophoblast metabolic regulators, particularly mTOR/IGF2, which are known to control placental amino-acid and lipid transporter function [33]. These molecular alterations, together with the region-specific differences in transporter expression observed in our model, likely contribute to the impaired vascular organization we identified [34]. The changes detected in system A transporters further align with their established role in supporting fetal amino-acid supply under nutritional stress [35,36]. Taken together, these pathways provide a plausible biological framework linking maternal protein restriction to the altered transporter profile, vascular remodeling, and fetal growth disturbances identified in our study.

To better understand the observed fetal growth patterns, it is important to note that LPD treatment in outbred mice did not affect feed intake or body weight in non-pregnant females. Moreover, during early pregnancy, maternal body weight changes remained undetectable, likely due to the relatively low protein demands of embryos compared to fetuses [37]. However, as gesta-

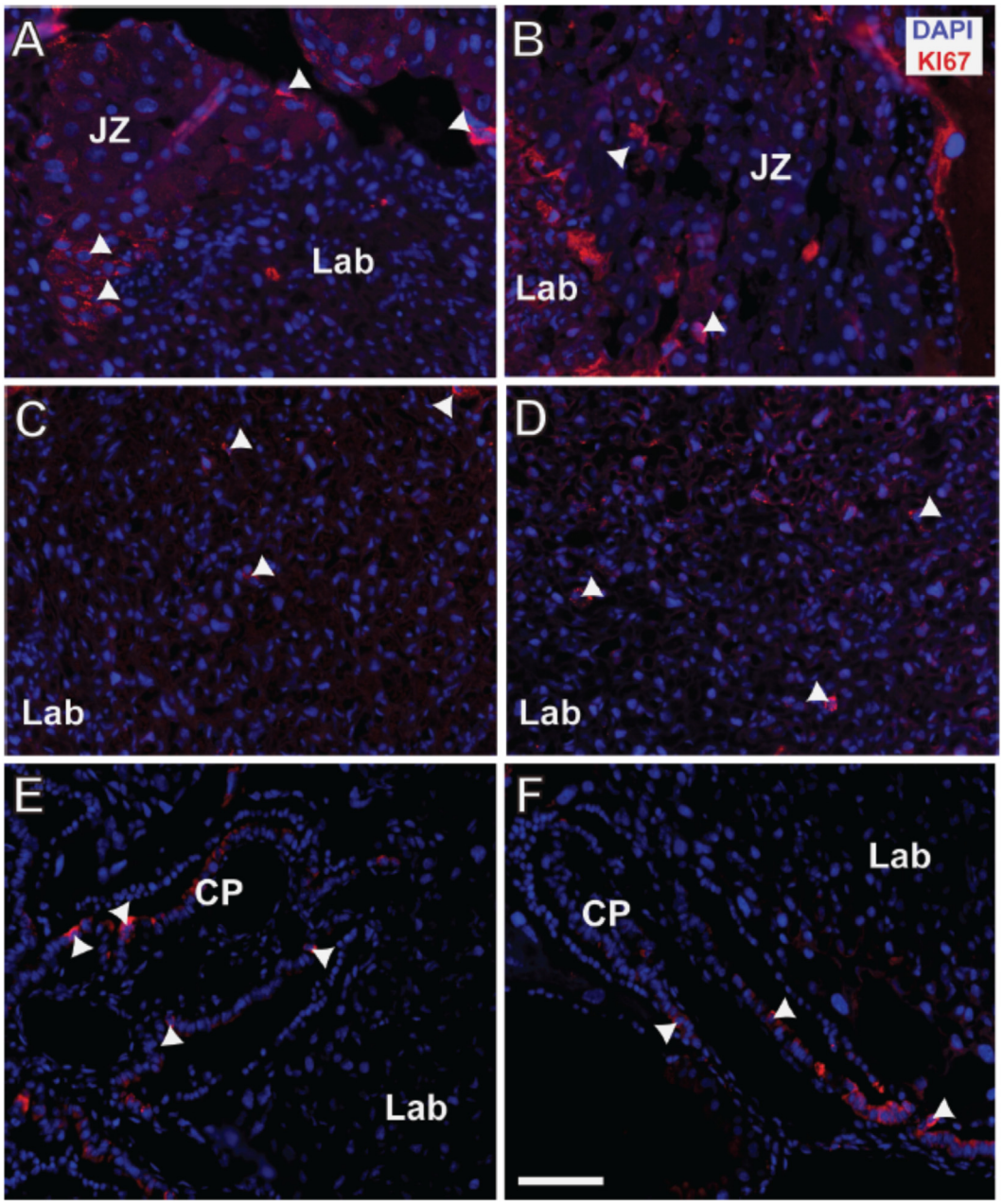

Fig. 5. Photomicrographs showing KI67 protein immunostaining in cells at the junctional zone (A–B), labyrinth-trophoblast (C–D) and chorionic plate (E-F) placental layers at GD 17.5 from normal (NPD: A, C, E, n=8) and low (LPD: B, D, F, n=10) protein intake females. White arrow heads indicate positive immunostaining to KI67 protein in cytoplasm, *i.e.*, proliferating cells. Cells were evaluated in the junctional zone (NPD: n= 976 cells/placenta; LPD: n= 707 cells/placenta), labyrinth trophoblast (NPD: n= 3,178 cells/placenta; LPD: n= 3,079 cells/ placenta) and chorionic plate (NPD: n= 926 cells/placenta; LPD: n= 966 cells/ placenta) placental layers. The scale bar indicates 50 μm and is representative for all photomicrographs. Abbreviations: CP, chorionic plate; JZ, junctional zone; Lab, labyrinth-trophoblast.

tion progressed, pregnant mice on LPD failed to assimilate sufficient protein during the fetal period. This deficiency was reflected in reduced maternal weight gain, despite higher feed and caloric intakes during late gestation.

LPD creates a suboptimal uterine nutritional environment for fetal development. However, as discussed by Díaz et al. [32], the placenta can recognize maternal nutritional status and regulate nutrient allocation to the fetus. This was evidenced by placental responses in the LPD group, which showed reduced weight and size, followed by adaptations in the labyrinth components. These adaptations included increased maternal sinusoids, decreased fetal vessels, and no changes of the interhemal membrane thickness. Furthermore, histomorphometrical evaluation of LPD placentae revealed that the junctional zone, an important region for pregnancy maintenance due to its glycogen and endocrine cells, did not show changes in cellular proliferation or cell death processes. In a similar biological and dietary context, Gonzalez et al. [7] used an inbred C57BL/6J mouse model and reported a reduction in the junctional zone in the placentae of dams subjected to 6% LPD. Comparable adaptations have also been reported in other animal models. In swine, for instance, LPD impaired placental angiogenesis and nutrient transfer, leading to IUGR and reduced litter survival [38,39]. In ruminants, protein restriction during gestation decreased placental vascularization and altered fetal muscle composition, which

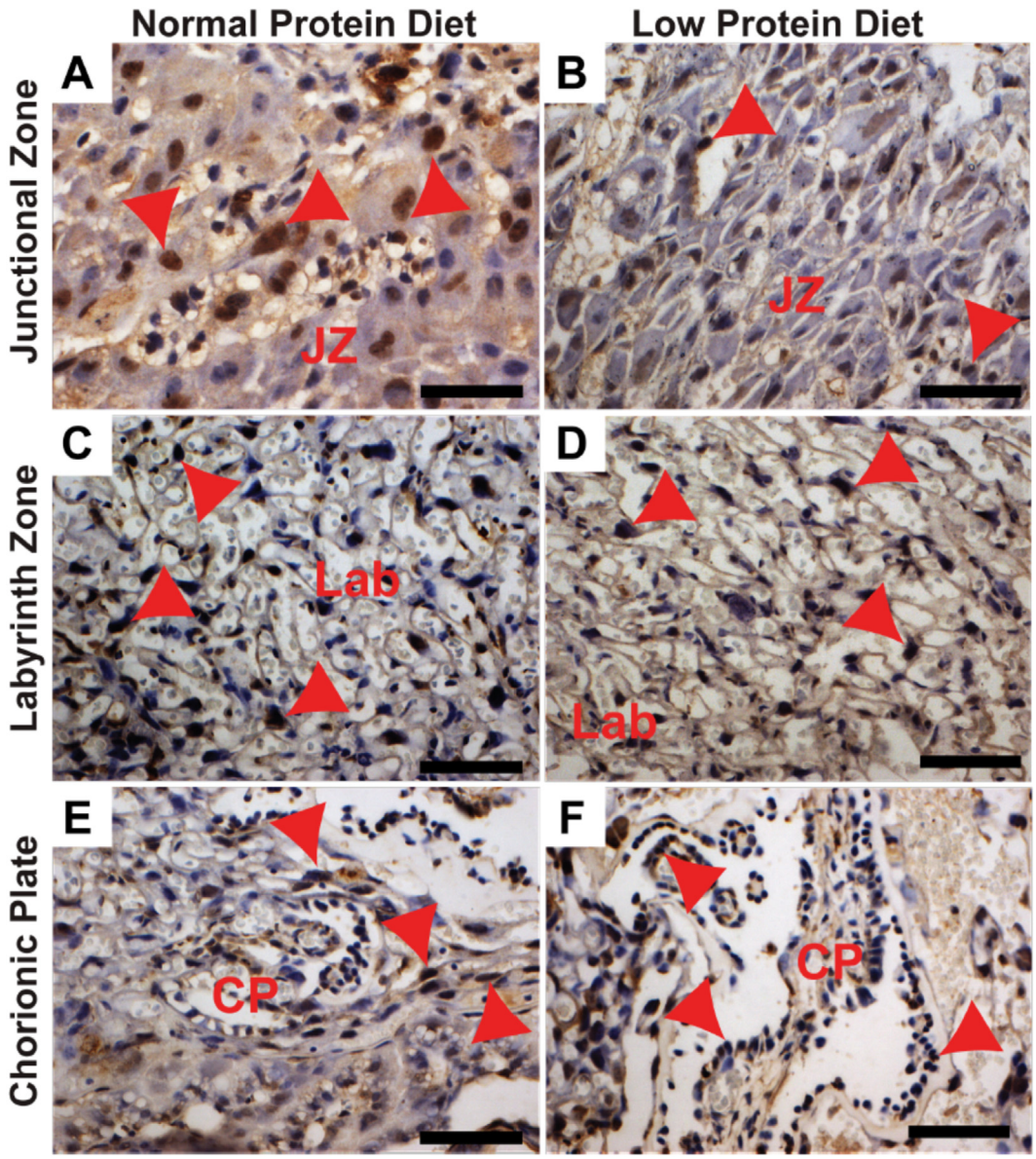

Fig. 6. Photomicrographs representing the TUNEL assay performed in the different placental layers from the normal (NPD, n=3) and low (LPD, n=5) protein intake experimental groups. The images depict the junctional zone (A-B), labyrinth-trophoblast (C-D) and chorionic plate (E-F) placental layers at GD 17.5 from normal (NPD: A; C; E) and low (LPD: B; D; F) protein intake females. Red arrow heads indicate TUNEL positive immunostaining, *i.e.*, cell death due to DNA fragmentation. Nuclei were evaluated in the junctional zone (NPD: n= 783 nuclei/placenta; LPD: n= 645 nuclei/placenta), labyrinth-trophoblast (NPD: n= 1,364 nuclei/placenta; LPD: n= 1,168 nuclei/placenta) and chorionic plate (NPD: n= 286 nuclei/placenta; LPD: n= 429 nuclei/placenta) placental layers. The scale bar indicates 60 μm and is representative for all photomicrographs. Abbreviations: CP, chorionic plate; JZ, junctional zone; Lab, labyrinth-trophoblast.

was linked to reduced offspring growth and long-term health risks [40,41]. Human studies also support these findings, as maternal protein undernutrition has been associated with impaired placental function, lower birth weights, and higher risks of metabolic disorders in adulthood [42] (Dutch famine cohort studies).These findings suggest that the observed results may be species-dependent and indicate that placentae exposed to specific levels of maternal LPD can undergo distinct morphofunctional adaptations to support pregnancy.

Our data provide evidence that under protein restriction, the placenta becomes smaller and exhibits fewer fetal vessels alongside proportionally enlarged maternal sinusoids, indicating compromised vascular organization for nutrient exchange. At the molecular level, the placenta adjusts its nutrient-sensing and transporter gene expression in a uterine-location–dependent manner, downregulating key metabolic regulators and lipid transporters in better-perfused regions (uterine edges) while upregulating amino acid transporters and compensatory pathways in more nutrient-limited regions (mid-uterus). Despite these adaptive responses, fetal growth remains impaired, particularly in males, which is evidenced by reduced fetal size, altered organ weights, and increased brain-to-liver weight ratios. Together, these findings show that maternal dietary protein restriction disrupts the diet–placenta–fetus relationship by altering placental morphology and functional markers. Although the placenta attempts to compensate, these adjustments partially meet fetal demands, resulting in measurable growth disturbances, especially in male offspring.

Table 4
Offspring and placenta biometrical outcomes at the late fetal period (GD17.5) and at birth according to gender after maternal normal (NPD) or low (LPD) protein intake

Parameters	NPD		LPD		*P*-value		
	Females	Males	Females	Males	Treatment effect	Sex effect	Treatment *sex
Late fetal period (GD17.5)							
N	42	46	37	41			
Fetuses/gender/litter (#)	4.20±0.60^{Aa}	4.60±0.60^{Aa}	5.30±0.80^{Aa}	5.80±0.80^{Aa}	.2508	NA	NA
Placental weight (g)	0.210±0.007^{Aa*}	0.220±0.006^{Aa*}	0.185±0.006^{Ba*}	0.170±0.007^{Ba*}	.0001	.7534	.0447
Fetal weight (g)	1.00±0.02^{Aa*}	1.10±0.02^{Ab*}	0.97±0.02^{Ba*}	0.98±0.02^{Ba*}	.0002	.0141	.0188
Placental size (mm)	10.3±0.3^{Aa}	10.8±0.3^{Aa}	9.0±0.3^{Ba}	9.0±0.3^{Ba}	.0001	.2988	.3633
Crown-rump length (mm)	21.8±0.3^{Aa}	23.0±0.3^{Ab}	21.4±0.3^{Ba}	21.7±0.3^{Ba}	.0034	.0061	.0942
Placental efficiency	5.0±0.2^{Aa}	5.2±0.2^{Ab}	5.4±0.2^{Ba}	5.8±0.2^{Bb}	.0015	.0349	.4563
Brain weight (g)	0.095±0.006^{Aa}	0.080±0.005^{Aa}	0.096±0.006^{Ba}	0.110±0.006^{Ba}	.0489	.8783	.0871
Liver weight (g)	0.070±0.002^{Aa}	0.075±0.003^{Aa}	0.063±0.003^{Ba}	0.058±0.003^{Ba}	.0001	.9091	.1170
Brain : liver weight ratio	1.40±0.10^{Aa*}	1.20±0.10^{Aa*}	1.80±0.20^{Ba*}	2.20±0.20^{Ba*}	.0001	.6228	.0297
Liver : body weight ratio	0.070±0.002^{Aa}	0.070±0.002^{Aa}	0.064±0.002^{Ba}	0.058±0.003^{Ba}	.0003	.1291	.4624
Newborn							
n	32	40	29	32			
Pups/gender/litter (#)	5.30±0.80^{Aa}	6.70±0.80^{Aa}	4.80±0.80^{Aa}	5.30±0.80^{Aa}	.8061	NA	NA
Birth weight (g)	1.65±0.03^{Aa}	1.66 0.03^{Aa}	1.64±0.03^{Aa}	1.65±0.03^{Aa}	.6778	.6000	.9177
Crown-rump length (mm)	31.2±0.2^{Aa}	31.7±0.2^{Aa}	31.0±0.2^{Aa}	31.3±0.2^{Aa}	.2410	.1197	.5964
Brain weight (g)	0.084±0.002^{Aa}	0.084±0.002^{Aa}	0.073±0.002^{Bb*}	0.082±0.002^{Ba*}	.0052	.0435	.0565
Liver weight (g)	0.072±0.002^{Aa}	0.070±0.002^{Aa}	0.060±0.002^{Ba}	0.055±0.002^{Ba}	.0001	.0873	.8332
Brain : liver weight ratio	1.20±0.04^{Aa}	1.20±0.04^{Ab}	1.30±0.08^{Ba}	1.50±0.07^{Ba}	.0022	.0188	.1038
Liver : body weight ratio	0.044±0.001^{Aa}	0.040±0.001^{Ab}	0.036±0.001^{Bb}	0.033±0.001^{Bb}	.0001	.0155	.9645

Abbreviation: NA, not applicable.
^{A,B} LSMeans with different superscripts show treatment effects (differences between NPD and LPD groups; $P<.05$).
^{a,b} LSMeans with different superscripts, comparing female and male, indicate only gender differences ($P<.05$).
* LSMeans comparing females and males, indicate treatment by gender interactions ($P<.05$).

In the present study, male placentas in the LPD group appeared more efficient than female placentas, producing more grams of fetus per gram of placenta (Table 4). Accordingly, one would expect fewer male fetuses in the 10th percentile in the LPD group (Fig. 7). Paradoxically, this was not the case, as we observed 22% of LPD males in the 10th percentile at GD17.5. However, by birth, the number of males in the 10th percentile had decreased substantially, whereas the number of LPD males in the 75th percentile increased from 0% at GD17.5 to 25% at birth. In contrast, females showed an increase in the 10th percentile at birth but not in the 75th percentile. These results are consistent with greater placental efficiency in the male placenta as indicated by the fetal-to-placental weight ratio. Even though there was a placental adaptation to meet fetal growth nutritional demands in LPD male fetuses, these adaptations were not sufficient to prevent adverse male phenotype. This may be related to the impaired dam weight-gain in late gestation, likely due to less maternal protein intake, which, regardless of the placental adaptation to meet fetal growth nutritional demands in LPD male fetuses, these adaptations were not sufficient to prevent adverse male phenotype.

As each animal in an outbred population is genetically unique, with varying intrinsic genetic capacities [43], body weight frequency according to gender was evaluated. It was observed that LPD male fetuses exhibited higher relative body weight frequencies below the 10th percentile, with no fetuses above the 90th percentile. According to Sharma et al. [25], this percentile range is indicative of IUGR. Interestingly, this scenario changed at birth, as the relative frequency of body weight below the 10th percentile was similar between LPD and NPD males, despite the inability of LPD male newborns to surpass the 90th percentile, suggesting an intrauterine catch-up growth of LPD males leading to normal birth weight. Importantly, it has been demonstrated that placentae from conceptus generated by *in vitro* fertilization (IVF) undergo an intrauterine catch-up growth and are born with normal weight compared to their naturally conceived counterparts [23,44], indicating that this phenomenon occurs in different stressful events in mice. In contrast, fetal and newborn LPD females had body weights comparable to their NPD counterparts. It is important to note that although maternal LPD did not affect the prenatal growth of female offspring, their livers were lighter.

To understand the placental strategies adopted to support fetal growth, placental gene expression was evaluated according to uterine placental location: near the ovary, middle of the uterine horn, and close to the uterine body, in response to LPD (Fig. 8). This approach was used as Raz et al. [30] reported differences in fetal and placental growth due to uterine vascularization. It has been reported that under normal conditions, fetuses and placentae located at the edges of the uterine horns acquired more favorable growth conditions associated with blood flow. However, placentae located in the middle of the uterine horn needed to develop adaptations for their own development [30]. This evaluation highlighted the placental strategies aiming to better support fetal growth within a litter in normal conditions. In response to LPD, we reported modified expressions of the nutrient sensor and the nutrient transport regulators in the placenta, *mTor* and *Igf2r*, alongside with altered expression of neutral amino acid transporters and *Kiss1R* (a regu-

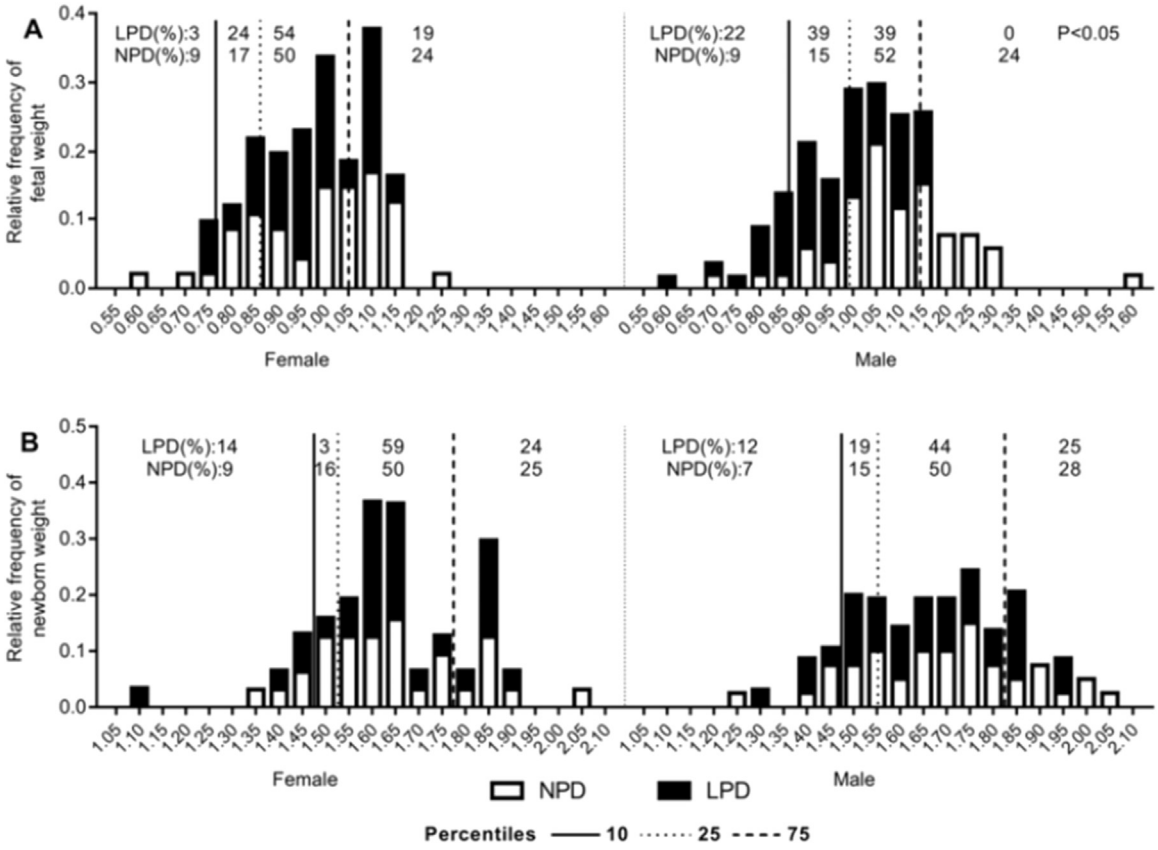

Fig. 7. Fetal (A) and newborn (B) relative body weight frequencies, according to gender, in normal (NPD) and low (LPD) protein offspring. White and black columns represent NPD and LPD experimental groups, respectively. Complete dotted and dashed lines represent the 10th, 25th and 75th percentiles, respectively. Below the 10th body weight percentile, the individuals present a higher risk of intrauterine growth impairments; between the 10th and 25th body weight percentiles, offspring is considered low body weight; the range between the 25th and 75th body weight percentiles represent adequate body weight; beyond the 75th body weight percentile stands the above normal weight non-obese individuals. In this analysis, 100 female fetuses (NPD: n=47; LPD: n=53), 110 male fetuses (NPD: n=52; LPD: n=58), 61 female newborns (NPD: n=32; LPD: n=29) and 72 male newborns (NPD: N=40; LPD: N=32) were used. The relative percentages (%) are represented for each percentile interval. Body weight frequency in females was not affected by LPD (P=.4231), but higher prevalence of LPD male fetuses below the 10th and 25th body weight percentiles and none above the 75th were observed (P=.0457). At birth, both LPD males (P=.1565) and females (P=.4368) showed similar body weight frequency compared to their NPD counterparts.

lator of placentation and angiogenesis; [45]), that represented placental strategies to modulate its development (size, weight, and fetal vessel proportion) to adjust fetal growth to the availability of nutrients and oxygen imposed by differences in intrauterine location. In response to LPD, near the ovary, placentae showed down-regulation of *Fatp4, Mtor*, and *Kiss1*, which generally would indicate reduced lipid absorption and moderate nutrient transport to the fetus [46,47], probably as a result of greater blood flow to the uterine horn-edges [30,48]. At the same time, *Stat3* was up regulated, suggesting an adaptive response aiming to increase overall nutrient transfer and assure placental cellular survival and proliferation [49]. In the middle of the uterine horns, which receives less uterine blood flow, LPD down regulated *Snat4* expression, while upregulating *Snat1 and Kiss1*, potentially reflecting an effort to enhance/adjust amino acid uptake and placentation to lower uterine blood-flow and LPD [47]. Close to the cervix, *Igf2r* was down-regulated, whereas *Snat1* and *Kiss1r* were up-regulated in response to LPD, indicating a compensatory mechanism to improve/adjust amino acid transport and placentation [47,48,50], even though it has been reported greater blood flow in the uterine edges than in the middle of the uterine horn–suggesting that uterine blood flow must not be the sole modulator of regulatory genes involved with nutrient transport in the placenta in response to LPD. These findings show that LPD placentae attempt to counteract nutritional challenges by modulating gene expression based on their uterine location, though their ability to maintain essential metabolic and growth functions varies across regions. Currently, one limitation of the present findings stands in the fact that we did not undertake protein expression analysis and functional experiments to address whether protein expression and the actual placental transport of glucose, aminoacids and lipids would be altered in LPD pregnancies, in a uterine location dependent manner. This clearly requires further investigation.

In all uterine locations, the IFG2-IGF2R axis and the Kisspeptin/Kiss1R system in LPD placentae were affected. The IFG2-IGF2R axis is essential for controlling the expansion of placental vasculature in late pregnancy [34], and its endocrine function regulates nutrient distribution to the fetus, thereby controlling protein synthesis and energy metabolism [51]. Although studies examining placental function related to the Kisspeptin/Kiss1R system during the final third of pregnancy in mice are scarce, research in pregnant women has shown that increased expression of this system is associated with hypertensive disorders of pregnancy and fetal growth restriction in the last trimester [52]. Conversely, low levels of kisspeptin have been linked to fetal growth restriction and miscarriage [53,54]. Given that the Kisspeptin/KISS1R system regulates trophoblast invasion, embryo implantation, placentation, and early pregnancy [55], our results suggest that LPD modifies its expression in a uterine location–dependent manner. Further studies are needed to clarify

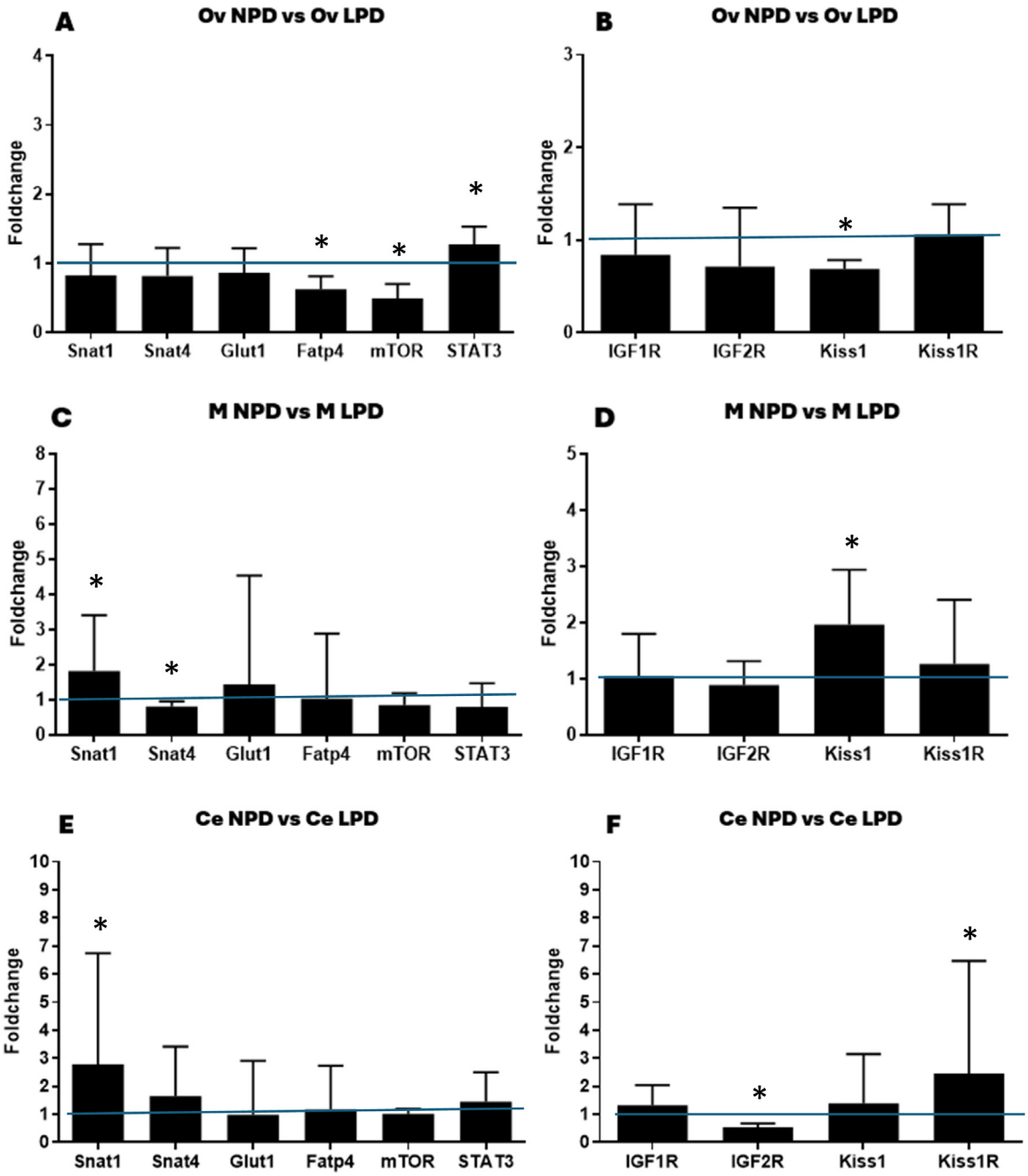

Fig. 8. Relative gene expression of placental nutrient transporters, metabolic regulators, placental growth factors and kisspeptin according to placental location performed with a pool of 3 placentas of 3 different dams from the normal (NPD) and low (LPD) protein intake experimental groups. *Ov*: near the ovary (A, B); *M*: middle portion of the uterus (C, D); *Ce:* close to the uterine body (E, F). The straight line coming from the number 1 in the Y axis represents the NPD group. *Indicates statistical difference ($P<.05$). Abbreviations: *Fatp4(Slc27a4)*, Fatty acid transporter-4; *Glut1(Slc2a1)*, Glucose transporter-1; *Igf1r*, Insulin-like growth factor-1 receptor; *Igf2r*, Insulin-like growth factor-2 receptor; *Kiss1 (Kiss-1 metastasis-suppressor)*, Kisspeptin; *Kiss1r*, Kisspeptin receptor; *Mtor*, Mammalian target of rapamycin**;** *Snat1(Slc38a1)*, Sodium-coupled neutral amino acid transporter-1; *Snat4(Slc38a1)*, Sodium-coupled neutral amino acid transporter-4; *Stat3***,** Signal transducer and activator of transcription-3**.**

the specific role of this system in placentation during the final third of pregnancy in mice.

In fact, the placental adaptations in response to LPD were sufficient to promote normal birthweight, despite the *in utero* lower weight detected. Similarly, Appel et al. [56] reported a glucose-driven intrauterine catch-up growth in an obese mouse model that occurred between GD15.5 and 18.5. In contrast, our findings indicate that growth recovery occurred later––between GD17.5 and birth and significantly reduced the frequency of newborns weighing below the 10th percentile. Given that gestational undernutrition is a key driver of metabolic programming later in life [44], future studies should explore the long-term and transgenerational consequences of placental adaptations to a low-protein diet (LPD) in adult outbred progeny.

Collectively, our morphological results demonstrate that although LPD impairs the proportion of fetal vessels in the placenta, reductions in placental weight and size occur without affecting cell proliferation, and cell death processes. Despite these adaptations, fetal growth is temporarily impaired between GD17.5 and birth, warranting further investigation into whether this transient growth

disorder may lead to long term postnatal impairments, consistent with the DOHAD hypothesis. Moreover, the altered gene expression profile highlights the mechanisms by which the placenta adapts to LPD and supports fetal growth recovery until birth.

Data availability statement

The data that support this study will be shared upon reasonable request to the corresponding author.

CRediT authorship contribution statement

Fernando Felicioni: Writing – original draft, Validation, Methodology. **José Andrés Nivia-Riveros:** Writing – original draft, Methodology. **Andre Lucas Caldeira-Brant:** Methodology, Formal analysis. **Thais de Mérici Domingues e Paula:** Methodology, Conceptualization. **Lucas Carvalho Cardoso:** Methodology, Formal analysis. **Camila Ferreira Sales:** Methodology, Formal analysis. **Julia Meireles Nogueira:** Methodology, Formal analysis. **Ana Maria Alvarenga Fagundes:** Methodology. **Elizete Rizzo:** Validation, Formal analysis. **Hélio Chiarini-Garcia:** Writing – review & editing, Methodology, Data curation. **Erika Cristina Jorge:** Writing – review & editing, Methodology, Formal analysis. **Enrrico Bloise:** Writing – review & editing, Validation, Methodology, Formal analysis. **Fernanda Radicchi Campos Lobato de Almeida:** Writing – review & editing, Validation, Supervision, Methodology, Formal analysis, Conceptualization.

Acknowledgments

The authors thank Prof. Estela Bevilacqua, from the Instituto de Ciências Biológicas (USP), for her scientific advice. Part of the microscopic data shown in this work was obtained using the equipment from the Centro de Aquisição e Processamento de Imagens (CAPI) from the Institute of Biological Sciences of the Federal University of Minas Gerais.

Declaration of competing interests

The authors declare no conflicts of interest.

Funding

Financial support for this study was provided by, Conselho Nacional de Desenvolvimento Científico e Tecnologico (CNPq/INCT DOHaD 409165/2024-7); Coordenação de Aperfeiçoamento de Pessoal de Nível Superior-Brasil (CAPES), and Fundação de Amparo à Pesquisa do Estado de Minas Gerais (FAPEMIG). F.F. and J.A.N.R. were funded by CAPES (Finance code 001). E.B. is funded by CNPq (310489/2023-7) and FAPEMIG (00338-18 and APQ-00099-24); E.C.J. by CNPq (304437/2022-0), and F.R.C.L.A. by CNPq (312050/2022-4).

References

[1] Jiang W, Zhao Y, Wu X, Du Y, Zhou W. Health inequalities of global protein-energy malnutrition from 1990 to 2019 and forecast prevalence for 2044: data from the global burden of disease study 2019. Public Health 2023;225:102–9. doi:10.1016/j.puhe.2023.10.003.
[2] Herring CM, Bazer FW, Johnson GA, Wu G. Impacts of maternal dietary protein intake on fetal survival, growth, and development. Exp Biol Med (Maywood) 2018;243(6):525–33. doi:10.1177/1535370218758275.
[3] World Health Organization (2019) United nations decade of action on nutrition. World Health Organization. https://www.who.int/nutrition/decade-of-action/en/. [accessed 18 April 2019]
[4] Connor KL, Kibschull M, Matysiak-Zablocki E, Nguyen TTN, Matthews SG, Lye SJ, et al. Maternal malnutrition impacts placental morphology and transporter expression: an origin for poor offspring growth. J Nutr Biochem 2020;78:108329. doi:10.1016/j.jnutbio.2019.108329.
[5] Rutland CS, Latunde-Dada AO, Thorpe A, Plant R, Langley-Evans S, Leach L. Effect of gestational nutrition on vascular integrity in the murine placenta. Placenta 2007;28:734–42. doi:10.1016/j.placenta.2006.07.001.
[6] Gao H, Yallampalli U, Yallampalli C. Gestational protein restriction affects trophoblast differentiation. Front Biosci (Elite Ed) 2013;5:591–601. doi:10.2741/e641.
[7] Gonzalez PN, Gasperowicz M, Barbeito-Andrés J, Klenin N, Cross JC, Hallgrímsson B. Chronic protein restriction in mice impacts placental function and maternal body weight before fetal growth. PLoS One 2016;11:1–18. doi:10.1371/journal.pone.0152227.
[8] Burton GJ, Fowden AL, Thornburg KL. Placental origins of chronic diseases. Physiol Rev 2016;96:1509–65. doi:10.1152/physrev.00029.2015.
[9] Dimasuay KG, Boeuf P, Powell TL, Jansson T. Placental responses to changes in the maternal environment determine fetal growth. Front Physiol 2016;7:12. doi:10.3389/fphys.2016.00012.
[10] Lo JO, Schabel MC, Gaffney J, Lewandowski KS, Kroenke CD, Roberts C Jr, et al. Impaired placental hemodynamics and function in a non-human primate model of gestational protein restriction. Sci Rep 2023;13:841. doi:10.1038/s41598-023-28051-y.
[11] He T, Yuan Z, Chen Q, Luo J, Mao J, Yang Y, et al. Circular RNAs mediate the regulation of maternal placental nutrient transport and fetal development by sugar-sweetened beverages. Food Res Int 2024;193:114856. doi:10.1016/j.foodres.2024.114856.
[12] Paula TMD, Cardoso LC, Felicioni F, Caldeira-Brant AL, Santos TG, Castro-Oliveira H, et al. Maternal chronic caffeine intake impairs fertility, placental vascularization and fetal development in mice. Reprod Toxicol 2023;121:108471. doi:10.1016/j.reprotox.2023.108471.
[13] Tuttle AH, Philip VM, Chesler EJ, Mogil JS. Comparing phenotypic variation between inbred and outbred mice. Nat Methods 2018;15:994–6. doi:10.1038/s41592-018-0224-7.
[14] Cardoso LC, Costa BFMD, Felicioni F, Oliveira DR, Caliari MV, Bloise E, et al. Maternal protein restriction before and during pregnancy leads to a gestational day-dependent response of folliculogenesis in outbred mice. Reprod Fertil Dev 2021. doi:10.1071/RD21028.
[15] Ito T, Hoshiai K, Tanabe K, Nakamura A, Funamoto K, Aoyagi A, et al. Maternal undernutrition with vaginal inflammation impairs the neonatal oligodendrogenesis in mice. Tohoku J Exp Med 2011;223:215–22. doi:10.1620/tjem.223.215.
[16] Ajayi AF, Akhigbe RE. Staging of the estrous cycle and induction of estrus in experimental rodents: an update. Fertil Res Pract 2020;6(5):1–15. doi:10.1186/s40738-020-00074-3.
[17] Bertolin K, Murphy BD. Reproductive tract changes during the mouse estrous cycle. The guide to investigation of mouse pregnancy. Croy BA, Yamada AT, DeMayo FJ, Adamson SL, editors. 1st ed., Amsterdam: Elsevier; 2014. p85-94. doi:10.1016/B978-0-12-394445-0.00007-2.
[18] Goldman JM, Murr AS, Cooper RL. The rodent estrous cycle: characterization of vaginal cytology and its utility in toxicological studies. Birth Defects Res B Dev Reprod Toxicol 2007;80(2):84–97. doi:10.1002/bdrb.20106.
[19] Oteyola AO, Oliveira IMS, Almeida JM, Cardoso LC, Paula TMDE, Nogueira JM, et al. Chronic fat consumption affects metabolic aspects of murine physiology and influences ovarian follicle atresia. Reprod Toxicol 2025;132:108836. doi:10.1016/j.reprotox.2025.108836.
[20] Reeves PG, Nielsen FH, Fahey CG Jr. AIN-93 purified diets for laboratory rodents: final report of the American institute of nutrition ad of the AIN-76A rodent diet. J Nutr 1993;123:1939–51. doi:10.1093/jn/123.11.1939.
[21] Chiarini-Garcia H, Parreira GG, Almeida FRCL. Glycol methacrylate embedding for improved morphological, morphometrical, and immunohistochemical investigations under light microscopy: tests as a model. Methods Mol Biol 2011;689:3–18. doi:10.1007/978-1-60761-950-5_1.
[22] Pang SC, Janzen-Pang J, Tse MY, Croy BA, Lima PDA. The cycling and pregnant mouse: gross anatomy. In: 'The guide to investigation of mouse pregnancy'. Amsterdam, NL: Elsevier; 2014. p. 3–19. (Eds Croy BA, Yamada AT, DeMayo FJ, Adamson SL).
[23] Bloise E, Lin W, Liu X, Simbulan R, Kolahi KS, Petraglia F, et al. Impaired placental nutrient transport in mice generated by in vitro fertilization. Endocrinology 2012;153:3457–67. doi:10.1210/en.2011-1921.
[24] Hayward CE, Lean S, Sibley CP Jones RL, Wareing M, Greenwood SL, Dilworth MR. Placental adaptation: what can we learn from birthweight: placental weight ratio? Front Physiol 2016;7:1–13. doi:10.3389/fphys.2016.00028.
[25] Sharma D, Shastri S, Sharma P. Intrauterine growth restriction: antenatal and postnatal aspects. Clin Med Insights Pediatr 2016;10:67–83. doi:10.4137/CMPed.S40070.
[26] Christiansen S, Boberg J, Axelstad M, Dalgaard M, Vinggaard AM, Metzdorff SB, et al. Low-dose perinatal exposure to di(2-ethylhexyl) phthalate induces anti-androgenic effects in male rats. Reprod Toxicol 2010;30:313–21. doi:10.1016/j.reprotox.2010.04.005.
[27] Chiarini-Garcia H, Meistrich ML. High-resolution light microscopic characterization of spermatogonia. Methods Mol Biol 2008;450:95–107. doi:10.1007/978-1-60327-214-8_6.
[28] Bozzola J, Russel L. Quantitative electron microscopy. in 'electron microscopy: principles and techniques for biologists. Sudbury, Massachusetts, USA: Jones and Bartlett Publishers; 1999. p. 320–41. (Eds J Bozzola, L Russel).
[29] Drumond AL, Meistrich ML, Chiarini-Garcia H. Spermatogonial morphology and kinetics during testis development in mice: a high-resolution light microscopy approach. Reproduction 2011;142:45–155. doi:10.1530/REP-10-0431.

[30] Raz T, Avni R, Addadi Y, Cohen Y, Jaffa AJ, Hemmings B, et al. The hemodynamic basis for positional- and inter-fetal dependent effects in dual arterial supply of mouse pregnancies. PLoS One 2012;7(12):e52273. doi:10.1371/journal.pone.0052273.
[31] Pfaffl MW, Horgan GW, Dempfle L. (Relative Expression Software Tool (REST©) for Group-wise Comparison and Statistical Analysis of Relative Expression Results in Real-Time PCR). 30. 2002. doi:10.1093/nar/30.9.e36.
[32] Díaz P, Powell TL, Jansson T. The role of placental nutrient sensing in maternal-fetal resource allocation. Biol Reprod 2014;91:1–10. doi:10.1095/biolreprod.114.121798.
[33] Jansson T, Aye IL, Goberdhan DC. The emerging role of mTORC1 signaling in placental nutrient-sensing. Placenta 2012;v.33(Suppl 2):e23–9 Suppl 2. doi:10.1016/j.placenta.2012.05.010.
[34] Sandovici I, Georgopoulou A, Pérez-García V, Hufnagel A, López-Tello J, Lam BYH, et al. The imprinted Igf2-Igf2r axis is critical for matching placental microvasculature expansion to fetal growth. Dev Cell 2022;57:63–79 e8. doi:10.1016/j.devcel.2021.12.005.
[35] Desforges M, Mynett KJ, Jones RL, Greenwood SL, Westwood M, Sibley CP, et al. The SNAT4 isoform of the system an amino acid transporter is functional in human placental microvillous plasma membrane. J Physiol 2009;15(1):61–72 587. doi:10.1113/jphysiol.2008.161331.
[36] Desforges M, Greenwood SL, Glazier JD, Westwood M, Sibley CP. The contribution of SNAT1 to system a amino acid transporter activity in human placental trophoblast. Biochem Biophys Res Commun 2010;16(1):130–4 398. doi:10.1016/j.bbrc.2010.06.051.
[37] Regnault TRH, Friedman JE, Wilkening RB, Anthony RV, Hay WW Jr. Fetoplacental transport and utilization of amino acids in IUGR–a review. Placenta 2005;26(Suppl A):S52–62. doi:10.1016/j.placenta.2005.01.003.
[38] Li XL, Bazer FW, Johnson GA, Burghardt RC, Frank JW, Dai ZL, et al. Dietary supplementation with L-arginine between days 14 and 25 of gestation enhances embryonic development and survival in gilts. Amino Acids 2014;46:375–84.
[39] Wu G, Bazer FW, Burghardt RC, Johnson GA, Kim SW, Li XL, et al. Impacts of amino acid nutrition on pregnancy outcome in pigs: mechanisms and implications for swine production. J Anim Sci 2010;88:E195–204.
[40] Micke GC, Sullivan TM, Soares Magalhaes RJ, Rolls PJ, Norman ST, Perry VEA. Heifer nutrition during early- and mid-pregnancy alters fetal growth trajectory and birth weight. Anim Reprod Sci 2010;117(1):1–10. doi:10.1016/j.anireprosci.2009.03.010.
[41] Mossa F, Carter F, Walsh SW, Kenny DA, Smith GW, Ireland JLH, et al. Maternal undernutrition in cows impairs ovarian and cardiovascular systems in their offspring. Biol Reprod 2013;88(4):1–9. doi:10.1095/biolreprod.112.107235.
[42] Switkowski KM, Jacques PF, Must A, Hivert MF, Fleisch A, Gillman MW. Higher maternal protein intake during pregnancy is associated with lower cord blood concentrations of insulin-like growth factor (IGF)-II, IGF binding protein 3, and insulin, but not IGF-I, in a cohort of women with high protein intake. J Nutr 2017:1392–400.
[43] Gatti DM, Svenson KL, Shabalin A, Wu LY, Valdar W, Simecek P, et al. Quantitative trait locus mapping methods for diversity outbred mice. G3 (Bethesda) 2014;4:1623–33. doi:10.1534/g3.114.013748.
[44] Bloise E, Feuer SK, Rinaudo PF. Comparative intrauterine development and placental function of ART conceptuses: implications for human reproductive medicine and animal breeding. Hum Reprod Update 2014;20:822–39. doi:10.1093/humupd/dmu032.
[45] Musa E, Salazar-Petres E, Vatish M, Levitt N, Sferruzzi-Perri AN, Matjila MJ. Kisspeptin signaling and its correlation with placental ultrastructure and clinical outcomes in pregnant South African women with obesity and gestational diabetes. Placenta 2024;154:49–59. doi:10.1016/j.placenta.2024.05.138.
[46] Lager S, Powell TL. Regulation of nutrient transport across the placenta. J Pregnancy 2012:179827 2012. doi:10.1155/2012/179827.
[47] Panting EN, Weight JH, Sartori JA, Coall DA, Smith JT. The role of placental kisspeptin in trophoblast invasion and migration: an assessment in *Kiss1r* knockout mice, BeWo cell lines and human term placenta. Reprod Fertil Dev 2024;36:RD23230. doi:10.1071/RD23230.
[48] Bloise E, Braga JRS, Andrade CBV, Imperio GE, Martinelli LM, Antunes RA, et al. Altered umbilical cord blood nutrient levels, placental cell turnover and transporter expression in human term pregnancies conceived by intracytoplasmic sperm injection (ICSI). Nutrients 2021;13(8):2587. doi:10.3390/nu13082587.
[49] Marzioni D, Piani F, Di Simone N, Giannubilo SR, Ciavattini A, Tossetta G. Importance of STAT3 signaling in preeclampsia (Review). Int J Mol Med 2025;55(4):58. doi:10.3892/ijmm.2025.5499.
[50] Constancia M, Angiolini E, Sandovici I, Smith P, Smith R, Kelsey G, et al. Adaptation of nutrient supply to fetal demand in the mouse involves interaction between the Igf2 gene and placental transporter systems. Proc Natl Acad Sci USA 2005;102(52):19219–24. doi:10.1073/pnas.0504468103.
[51] Lopez-Tello J, Yong HEJ, Sandovici J, Dowsett GKC, Christoforou ER, Salazar-Petres E, et al. Fetal manipulation of maternal metabolism is a critical function of the imprinted Igf2 gene. Cell Metab 2023;35(7):. e6. doi:10.1016/j.cmet.2023.06.007.
[52] Abbara A, Al-Memar M, Phylactou M, Daniels E, Patel B, Eng PC, et al. Changes in circulating kisspeptin levels during each trimester in women with antenatal complications. J Clin Endocrinol Metabol 2022;107(1):e71–83. doi:10.1210/clinem/dgab617.
[53] Armstrong RA, Reynolds RM, Leask R, Shearing CH, Calder AA, Riley SC. Decreased serum levels of kisspeptin in early pregnancy are associated with intra-uterine growth restriction and pre-eclampsia. Prenat Diagn 2009;29:982–5. doi:10.1002/pd.2328.
[54] Tsoutsouki J, Patel B, Comninos AN, Dhillo WS, Abbara WS. Kisspeptin in the prediction of pregnancy complications. Front Endocrinol (Lausanne) 2022;13:942664. doi:10.3389/fendo.2022.942664.
[55] Hu KL, Chang HM, Zhao HC, Yu Y, Li R, Qiao J. Potential roles for the kisspeptin/kisspeptin receptor system in implantation and placentation. Hum Reprod Update 2019;25(3):326–43. doi:10.1093/humupd/dmy046.
[56] Appel S, Grothe J, Storck S, Janoschek R, Bae-Gartz I, Wohlfarth M, et al. A potential role for GSK3β in glucose-driven intrauterine catch-up growth in maternal obesity. Endocrinology 2018;160:377–86. doi:10.1210/en.2018-00899.